Assembly of Hydrophobic Shells and Shields around Lanthanides

Steven W. Magennis,[b] Simon Parsons,[b] and Zoe Pikramenou*[a]

Abstract: Luminescent lanthanide complexes have been developed, based on the assembly of bulky ligands around the lanthanide ion, to provide shell-type protection of the ion from coordinated solvent molecules. Aryl-functionalised imidodiphosphinate ligands (tpip and Metpip) provide a bidentate anionic site that leads to hexa-coordinate lanthanide complexes in which the aryl groups surround the ion. There are twelve phenyl groups around the lanthanide that act as "remote" (from the binding site) sensitisers for the metal ion. It is shown that these ligands are suitable for sensitising luminescence for *all* the lanthanides that emit in the visible range, namely, Sm^{III}, Eu^{III}, Tb^{III}, Dy^{III}. A "built-in" shield on the ligand is designed to provide a complete block of the approach of water to the lanthanide ion. The synthesis of the ligands and their lanthanides complexes as well as detailed photophysical studies of the complexes in solution and in the solid-state are presented.

Keywords: cages · lanthanides · luminescence · molecular devices · supramolecular chemistry

Introduction

Lanthanide(III) ions are popular luminescent centres with sharp f–f based emission at room temperature that ranges from the visible region to near-infrared. They do not absorb light efficiently; therefore, strong luminescence is triggered only by sensitisation of the lanthanide ion luminescence by coordinated organic ligands. A diverse range of associated applications have emerged that span the labelling of biomolecules to sensing and new display technologies.[1, 2] For light-conversion systems based on Ln^{3+} ions, the main requirements are high ligand-absorption coefficients, efficient ligand-to-metal energy transfer and minimal non-radiative deactivation of the excited state of the metal. Encapsulation of the Ln^{3+} ion by a polydentate/macrocyclic ligand (e.g. cryptands,[1, 3] calixarenes[4] and podands[5]) is the most common strategy employed to satisfy these criteria, particularly because it protects the lanthanide ion from water molecules that quench its luminescence.[6]

Instead of using pre-organised macrocyclic structures that encapsulate the ion, we are interested in the development of ligands that assemble around the lanthanide to form a hydrophobic shell. Our ligand design employs simple units, based on strong binding sites for lanthanide coordination and bulky aromatic groups, to play the dual role of antenna and solvent shield, and to thus form a hydrophobic shell around the metal ion. In this way, multi-step synthesis required to create macrocyclic structures is avoided. Additionally, the binding and antenna domains may be independent of each other to allow the sensitising group to be energetically optimised for a particular Ln^{3+} ion without changing the binding characteristics of the ligand (unlike those ligands in which the antennas are also the binding units, e.g. polypyridines,[1] benzimidazoles.[7] "Remote" light-harvesting units have been successfully employed to sensitise Ln^{3+} luminescence, though this was restricted to more intricate macrocyclic structures[8, 9]

[a] Dr. Z. Pikramenou
School of Chemical Sciences
The University of Birmingham
Edgbaston B15 2TT (UK)
Fax: (+44) 121 414 4446 or 4403
E-mail: z.pikramenou@bham.ac.uk

[b] S. W. Magennis, S. Parsons
Department of Chemistry, The University of Edinburgh
King's Buildings, West Mains Road, Edinburgh, EH9 3JJ (UK)

Supporting information for this article (excitation spectra of [Eu(tpip)$_3$], [Tb(tpip)$_3$], [Sm(tpip)$_3$] and [Tb(Metpip)$_3$]) is available on the WWW under http://www.chemeurj.org or from the author.

Abstract in Greek:

Σχηματίσθηκαν φωταυγή σύμπλοκα λανθανιδών με βάση την οργάνωση ογκωδών υποκαταστατών περί το ιόν του λανθανιδίου, κατά τέτοιο τρόπο ώστε να του παρέχουν ένα προστατευτικό κέλυφος προς αποφυγή συναρμογής μορίων διαλύτου. Αρυλοιμιδοδιφωσφινικοί υποκαταστάτες (tpip and Metpip) παρέχουν δισχιδή ανιοντική δομή, ώστε να σχηματίζουν εξάκις-υποκατεστημένα σύμπλοκα στα οποία οι αρυλομάδες περιβάλλουν το ιόν. Υπάρχουν δώδεκα φαινυλομάδες γύρω από κάθε ιόν λανθανιδίου, οι οποίες δρουν ως τηλε-ευαισθητοποιητές (απομακρυσμένοι από τη θέση συνδέσεως) για το μεταλλικό ιόν. Αποδεικνύεται ότι οι ανωτέρω υποκαταστάτες είναι κατάλληλοι για ενεργοποίηση της φωταύγειας σε όλες τις λανθανίδες Sm, Eu, Tb, Dy^{III} που εκπέμπουν στο ορατό. Η ενσωματωμένη ασπίδα στον υποκαταστάτη σχεδιάσθηκε ώστε να παρέχει πλήρη προστασία του ιόντος λανθανιδίου από την προσέγγιση μορίων ύδατος. Η εργασία παρουσιάζει τη σύνθεση των υποκαταστατών και τα σύμπλοκά τους με τις λανθανίδες, καθώς και λεπτομερείς φωτοφυσικές μελέτες των συμπλόκων σε διαλύματα και στη στερεά κατάσταση.

  0947-6539/02/0824-5761 $ 20.00+.50/0

We chose aryl-substituted imidodiphosphinates $[R_2P(O)NP(O)R_2]^-$ (R = Ph, tpip) as ligands that fit the requirements for our approach. Imidodiphosphinates can be viewed as inorganic analogues of β-diketonates, and it is well-known that the latter form luminescent lanthanide complexes.[10] However, imidodiphosphinates have a number of distinct advantages over β-diketonates with respect to their

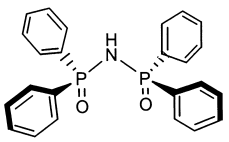
Htpip

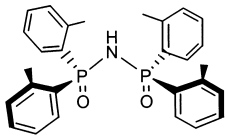
HMetpip

use as antenna ligands. Firstly, the chelating unit of tpip does not contain any O–H, C–H or N–H bonds (these bonds lead to non-radiative vibrational deactivation of the excited states of bound Ln^{3+} ions) unlike β-diketonates, which contain a C–H bond in the binding unit. Secondly, four aromatic groups can be attached to an imidodiphosphinate ligand (two on each phosphorus atom), whereas only two aromatic groups can be attached to a β-diketonate (one on each carbonyl carbon), allowing the imidodiphosphinate to collect a greater amount of light for a given chromophoric substituent. Thirdly, the bulkiness of each ligand (bearing four aryl groups) is important in our design as a shell to protect the lanthanide from water molecules; in contrast, β-diketonate lanthanide complexes have three open coordination sites for water molecules to bind and surfactant-like molecules have to be used in DELFIA immunoassay applications to increase their luminescence intensity and lifetime.[11] Finally, the aromatic substituents of a β-diketonate are in conjugation with the chelate, thereby affecting the excited-state properties of the light-harvesting unit. This can result in unpredictable changes of the sensitiser energy levels upon altering the light-harvesting units, and, in many cases, to strong ligand-to-metal charge-transfer bands that quench the lanthanide luminescence of the easily reduced lanthanides. In tpip-type ligands, the light-harvesting unit is "remote" from the binding site and it can be systematically modified to tune the emission properties of the lanthanide, thus avoiding the aforementioned problems.

A preliminary report of our work with tetraphenylimidodiphosphinate[12] introduced tpip as a new antenna ligand for europium and terbium ions to give highly luminescent, six-coordinate $[Ln(tpip)_3]$ complexes. This article gives a full account of the preparation and identification of complexes of tpip with Ln^{3+} ions that emit in the visible range (i.e., Ln = Sm, Eu, Tb, Dy), as well as the photophysical studies of these complexes in solution and in the solid state. We find that the lanthanide ion in these complexes is still partially susceptible to water binding. To circumvent this we have developed a new ligand, tetra-*o*-tolylimidodiphosphinic acid (HMetpip), that carries an additional built-in shield to fully encapsulate the lanthanide ion. The luminescent properties of the lanthanide complexes with Metpip are also described herein. We demonstrate that the extra shield leads to complete blocking of the approach of water molecules.

Results and Discussion

Preparation and characterisation of ligands: The ligand Htpip is prepared by the reaction of chlorodiphenylphosphine and hexamethyldisilazane followed by oxidation with H_2O_2.[13] Full spectroscopic characterisation of the ligand is undertaken as previous reports were incomplete. The FAB-MS of the ligand shows peaks at *m*/*z* 418 and 219, corresponding to $[M+H]^+$ and $[M-Ph_2PO+2H]^+$ respectively. The ^1H NMR spectrum of the ligand in $CDCl_3$ shows two multiplets at δ = 7.27–7.48 and 7.65–7.80 in a 3:2 ratio for the phenyl protons. The ^{31}P NMR spectrum in $CDCl_3$ shows a single resonance at $\delta = 21.0$, corresponding to two equivalent phosphorus atoms. It has been previously shown by X-ray crystallography[14] that this ligand crystallises in the tautomeric form N=P-OH. The molecules are linked, in infinite chains, by OH···O hydrogen bonds so that Htpip is insoluble in most solvents. This hydrogen bonding can only be overcome in strongly protic or basic media. To assess the light-absorbing properties of the ligand and the extent of conjugation in solution, the UV/Vis absorption spectrum was analysed. The structured band centred at $\lambda = 266$ nm for the Htpip sample is assigned to the characteristic long-wavelength $\pi \rightarrow \pi^*$ transition of ring-substituted benzene.[15] The position of this band is particularly affected by substituents that cause an increase in the conjugation of the benzene π-system. The observed absorption maximum suggests that this band can be attributed to a phosphorus-substituted benzene in which there is no conjugation of the phenyl groups with −P=N− in the binding unit.[16] In support of this, diphenylphosphinic acid, $[(C_6H_5)_2P(O)OH]$, in which there is obviously no −P=N− conjugation, shows the same spectral pattern as Htpip.[16] It should also be noted that the characteristic phenyl *B*-band in Htpip is situated at the tail end of a far more intense band at shorter wavelength, which can be attributed to the *K* band of the phenyl groups.

The preparation of the new ligand *N*-(*P*,*P*-di-2-methylphenylphosphinoyl)-*P*,*P*-di-2-methylphenyl-phosphinimidic acid (HMetpip), which is the *o*-tolyl analogue of Htpip, is accomplished in two steps (Scheme 1). The reagent chlorodi-2-methylphenylphosphine is prepared by the reaction of PCl_3 with the Grignard reagent of 2-bromotoluene.[17] Characterisation of chlorodi-2-methylphenylphosphine was performed by ^1H and ^{31}P NMR spectroscopy. Because of the sensitivity of this material, it was used immediately. The second step in Scheme 1 is the reaction of chlorodi-2-methylphenylphosphine and hexamethyldisilazane followed by oxidation with H_2O_2 to give pure HMetpip.

The FAB-MS of the HMetpip ligand shows an intense peak at *m*/*z* 474, corresponding to $[M+H]^+$. The ^1H NMR spectrum of the ligand in $CDCl_3$ shows multiplets corresponding to the phenyl protons and a singlet at $\delta = 2.18$ for the protons of the methyl group. The ^{31}P NMR spectrum, also in $CDCl_3$, shows one singlet at $\delta = 25.4$ for the equivalent phosphorus atoms of the ligand. As observed for Htpip, this ligand has a very low solubility in common organic solvents, and indeed is generally less soluble than Htpip. This suggests that, like Htpip, the ligand adopts a hydrogen-bonded structure in the solid state. The IR spectrum of HMetpip shows strong absorptions at $\tilde{\nu}$ =

0947-6539/02/0824-5762 $ 20.00+.50/0 *Chem. Eur. J.* **2002**, *8*, No. 24

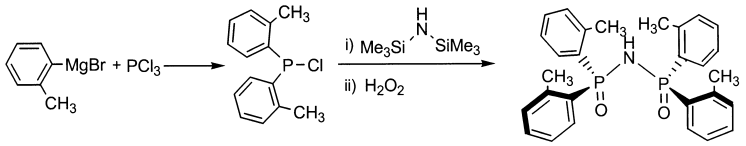

Scheme 1. Synthetic route to HMetpip.

1196, 1215 and 1229 cm^{-1}, characteristic of the vibrations of −P=N− systems, and strong absorptions at $\tilde{\nu} = 1068$ and 1094 cm^{-1} assigned to P–O stretching vibrations. These two sets of vibrations agree with those observed in many complexes of imidodiphosphinates, indicative of delocalisation of electron density in the solid-state structure of the free ligand.

The potassium salts of Ktpip and KMetpip, are prepared by dissolving the ligands in a methanolic KOH solution, removing the solvent and recrystallising the resultant white solid from ethanol to give the desired product. The FAB-MS of the products show peaks corresponding to $[M+H]^+$. The ^1H NMR spectra in CD_3OD show two multiplets corresponding to the phenyl protons, and an additional singlet at $\delta = 2.12$ for the protons of the methyl group of KMetpip. The ^{31}P NMR spectra show one singlet for the equivalent phosphorus atoms.

The crystal structure of KMetpip (Figure 1) is a hydrogen-bonded network with the formula $[K(Metpip)(MeOH)_2(H_2O)]_n$. One oxygen atom of each ligand is bonded directly to one K^+ ion and is hydrogen-bonded to a water molecule, while the other oxygen atom of the ligand is hydrogen-bonded

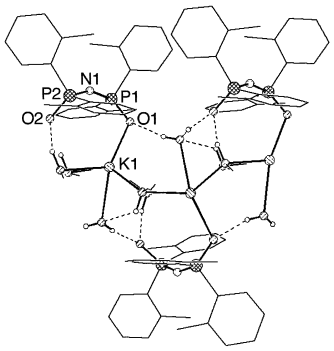

Figure 1. X-ray crystal structure of KMetpip showing the atomic numbering scheme; selected bond lengths [Å]: K1–O1 2.713(8), P1–O1 1.508(7), P1–N1 1.586(9), P2–N1 1.546(9), P2–O2 1.510(8).

to both a water and a MeOH molecule; the K^+ ion is bonded to the same MeOH molecule, another MeOH and a water. The network is formed by various additional interactions involving bridging solvent molecules, such as hydrogen bonding of the oxygen atom of adjacent ligands to the same water molecule. The P–N and P–O bond lengths of the imidodiphosphinate are short and are comparable to those found for the tpip complexes, indicative of electron delocalisation around the binding unit. The core of the hard donor sites is surrounded by the hydrophobic phenyl groups. The absorption spectra of KMetpip and Ktpip have similar profiles to those observed for the ligands.

Preparation and characterisation of lanthanide complexes: One equivalent of $LnCl_3 \cdot 6H_2O$ (Ln = Sm, Eu, Gd, Tb, Dy) was reacted with three equivalents of Ktpip[18] or KMetpip to afford good yields of the complexes $[Ln(tpip)_3]$ or $[Ln(Metpip)_3]$, respectively. These complexes are soluble in solvents, such as $CHCl_3$, CH_2Cl_2 and acetone, and are reasonably soluble in more polar solvents, such as acetonitrile. The Eu^{3+}, Tb^{3+}, Sm^{3+} and Dy^{3+} ions were chosen because these ions are all luminescent in the visible region.

The crystal structures of the europium and terbium complexes of Htpip were previously reported in our preliminary communication.[12] The unit cells revealed two types of symmetry around the metal: trigonal prismatic and distorted octahedral. We noticed a short van der Waals contact of a water molecule with the metal centre in the trigonal prismatic structure. This led us to the design of the methyl shield on the Metpip ligand as it was envisaged that the methyl groups would block the approach of the water molecule. The crystal structure of $[Eu(Metpip)_3]$ is shown in Figure 2. Three anionic

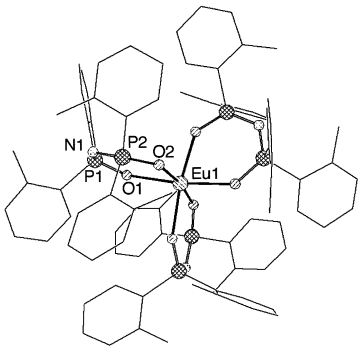

Figure 2. X-ray crystal structure of $[Eu(Metpip)_3]$ showing the atomic numbering scheme; selected bond lengths [Å: Eu1–O1 2.28(3), Eu1–O2 2.27(3), P1–O1 1.50(3), P2–O2 1.51(3), P1–N1 1.591(9), P2–N1 1.580(9).

Metpip ligands adopt a bidentate coordination mode to the Eu^{3+} ion to produce a six-coordinate metal ion as there are no coordinated solvent molecules (one $CHCl_3$ molecule per complex is found in the crystal lattice). The *o*-tolyl groups bound to the same P atom orient themselves such that the two methyl groups are pointing away from each other. There is evidence of CH–π interactions between protons of the methyl group and the phenyl rings in adjacent phosphorus atoms of the different ligands. As with the tpip structures, the low coordination number is attributed to the twelve *o*-tolyl groups that form a hydrophobic shell around the central metal ion. The average Eu–O bond length for the structure is 2.28 Å, with average P–N and P–O bond lengths of 1.59 and 1.51 Å, respectively, which compare well with those observed for $[Eu(tpip)_3]$. Six of the twelve methyl groups are located above the faces of the distorted octahedron defined by the oxygen atoms, shielding the approach of any solvent molecules.

  0947-6539/02/0824-5763 $ 20.00+.50/0

All complexes have been characterised by FAB-MS. The results confirm the complex formation, showing intense signals corresponding to $[M+H]^+$ and $[M-L]^+$ where L = tpip or Metpip for the respective complexes.

A full NMR study of the $[Ln(tpip)_3]$ complexes has been performed and the chemical shifts observed in the ^1H, ^{13}C and ^{31}P NMR spectra are summarised in Table 1. The NMR spectra of the complexes have broadly similar features, with the exception of the characteristic differences that arise from

Table 1. NMR data for $[Ln(tpip)_3]$.

Complex[a]	δ (^1H)	δ (^{13}C)	δ (^{31}P)
$[Sm(tpip)_3]$	7.58–7.66 (m, 24H; Ar)	131.1, 131.0, 130.9, 129.8	25.1 (s)
	7.19–7.26 (m, 12H; Ar)	127.5, 127.4, 127.3	
	7.03–7.08 (m, 24H; Ar)	[s, d, d, d]	
$[Eu(tpip)_3]$	7.48–7.54 (m, 24H; Ar)	129.8 (d, ^1J(P,C) = 137 Hz)	37.7 (s)
	7.21 (t, 12H; Ar)	129.4 (s)	
	6.95–6.99 (m, 24H; Ar)	128.9 (d, J(P,C) = 10 Hz)	
		127.0 (d, J(P,C) = 13 Hz)	
$[Tb(tpip)_3]$	7.97 (br s, 24H; Ar)	159.3 (br s, quart. C)	200.7 (s)
	7.35 (s, 12H; *p*-Ar)	134.5 (s)	
	6.28 (s, 24H; Ar)	130.4 (s)	
		128.6 (s)	
$[Dy(tpip)_3]$	8.1 (br s, 24H; Ar)	154 (br s, quart. C)	147.9 (s)
	7.45 (s, 12H; *p*-Ar)	132.6 (s)	
	6.57 (s, 24H; Ar)	130.2 (s)	
		128.3 (s)	

[a] $CDCl_3$ solvent at room temperature.

the magnetic properties of the different Ln^{3+} ions. In general, the chemical shifts arising from the interaction of ligand nuclei with a paramagnetic Ln^{3+} ion can be described in terms of two additive interactions: contact and pseudo-contact.[19] The pseudo-contact shift is caused by a through-space interaction between the electron and nuclear magnetic dipoles. The contact shift arises from covalent bonding interactions, where there is transfer of unpaired electron density onto the ligand. This effect is important for nuclei that are very close to the metal ion. Theoretical and experimental studies of paramagnetic lanthanide complexes can allow the relative magnitude and sign of the contact or pseudo-contact shifts for Ln^{3+} ions in a given complex to be deduced. The well-documented effect of Ln^{3+} ions on the NMR spectra of ligand nuclei will be used in a qualitative manner to aid characterisation of the $[Ln(tpip)_3]$ complexes.

Each of the complexes gives a ^1H NMR spectrum with three signals in a 2:1:2 ratio. These signals are very sharp multiplets for the Sm^{3+} and Eu^{3+} complexes whereas for the Tb^{3+} and Dy^{3+} complexes, each of them is broadened into a singlet. For the Dy^{3+} and Tb^{3+} complexes, the resonance at high frequency is especially broad and can be assigned to the *ortho* protons. These are nearest to the paramagnetic Ln^{3+} ion. Therefore, they would be expected to be more strongly affected than the *meta* and *para* protons, to which the other two signals can be attributed. These assignments suggest that each of the phenyl rings is equivalent; this is confirmed by the ^{13}C NMR spectra. For $[Eu(tpip)_3]$, seven signals are observed. This corresponds to three doublets, assigned to coupling between P and each of the quaternary, *ortho* and *meta* carbons, and a singlet that can be assigned to the *para* carbon. Similarly, the seven signals in the ^{13}C NMR spectrum of the Sm^{3+} complex must also be assigned to $^{31}P-^{13}C$ couplings; three doublets and one singlet. In this case, however, the peaks are too close together to identify them further. Similar $^{31}P-^{13}C$ couplings have been reported for complexes of tpip with Sn^{IV} where $^1J(P,C) \approx 139$ Hz, $^2J(P,C) \approx 11$ Hz and $^3J(P,C) \approx 14$ Hz.[20] Any fine structure is lost in the ^{13}C NMR spectra of the Dy^{3+} and Tb^{3+} complexes, as it was for the ^1H NMR spectra; four broad peaks are observed which are assigned to the quaternary, *ortho*, *meta* and *para* resonances, respectively. One peak, which is attributable to the quaternary carbon, is significantly shifted to higher frequency for the Tb^{3+} and Dy^{3+} complexes, and this agrees with the shifts for the *ortho* protons in the ^1H NMR spectra.

In the ^{31}P NMR spectrum of each of the complexes, a single resonance is obtained for all of the phosphorus atoms shifted to higher frequency with respect to the value of $\delta = 20.3$ reported[21] for the diamagnetic analogue $[Y(tpip)_3]$ due to the paramagnetic ion coordination. Broad ^{31}P NMR signals are observed for the Tb^{3+} and Dy^{3+} complexes, with large shifts to higher frequency. For a predominant pseudo-contact interaction, the ^{31}P signals of the Tb^{3+} and Dy^{3+} complexes would be expected to show large shifts in one direction, the Sm^{3+} complex would shift a small amount in the same direction and the Eu^{3+} complex would show shifts in the opposite direction.[22] If the contact interaction predominates, the order of ^{31}P shifts to higher frequency should be Tb > Dy > Eu > Sm, as observed for the tpip complexes.

These results provide good evidence that there is only one species in solution, with a single ligand environment. The possibility that a dynamic equilibrium (that is fast on the NMR timescale) exists between free and complexed ligand was also examined. The ^1H and ^{31}P NMR spectra of a mixture of $[Eu(tpip)_3]$ and $[Tb(tpip)_3]$ show only those signals observed for the original pure samples, which rules out the possibility of a fast exchange process. In support of this, the only changes that occur in the ^{31}P NMR spectrum of $[Tb(tpip)_3]$ in $[D_6]$acetone on cooling the solution from 297 to 240 K, is a slight broadening and a shift from $\delta = 207$ to 270. Such temperature-dependent shifts are not uncommon for lanthanide complexes.[19] Similarly, the ^{31}P NMR spectrum of $[Eu(tpip)_3]$ in CD_2Cl_2 at 297 K shows a singlet at $\delta = 39.8$, and at 260 K it shows a singlet at $\delta = 39.6$. This further evidence confirms that the only species which exists in solution is $[Ln(tpip)_3]$.

The ^1H NMR spectrum of $[Eu(Metpip)_3]$ in $CDCl_3$ shows two multiplets, in a 1:1 ratio, for the aromatic protons at $\delta =$ 7.15–7.16 and 6.10–6.31 and a singlet for the methyl protons at $\delta = 3.06$. In the ^{31}P NMR spectrum of the same sample, a single resonance is obtained at $\delta = 25.7$ for all of the phosphorus atoms. As $[Tb(Metpip)_3]$ was less soluble in $CDCl_3$ than $[Eu(Metpip)_3]$, only a ^{31}P NMR spectrum was obtained. Although this spectrum is weak, a broad singlet at $\delta = 142$ is clearly observed. As expected, the patterns and lanthanide-induced shifts observed in the $[Ln(Metpip)_3]$ NMR spectra are in agreement with NMR data for the corresponding $[Ln(tpip)_3]$ complexes.

The IR spectra of these complexes show strong absorptions assigned to P–O and P-N-P stretching vibrations. For both

  0947-6539/02/0824-5764 $ 20.00+.50/0 *Chem. Eur. J.* **2002**, *8*, No. 24

[Eu(Metpip)$_3$] and [Tb(Metpip)$_3$], these occur at 1224 and 1195 cm^{-1} [$\tilde{\nu}$(P-N-P)] and 1098 and 1071 cm^{-1} [$\tilde{\nu}$(P–O)]. These absorptions are similar to those observed for the free ligand, and are probably caused by hydrogen bonding in the latter molecule. The lack of absorbance in the region between 3100 and 4000 cm^{-1} suggests that there are no H_2O or MeOH molecules coordinated to the Ln^{3+} ion.

Photophysical studies of lanthanide complexes of tpip: The absorption spectrum of [Eu(tpip)$_3$] in CH_3CN (Figure 3a) has a structured band centred at 270 nm ($\lambda_{max} = 265$ and 272 nm) on the tail of an intense band at a shorter wavelength; the absorption profile in $CHCl_3$ is identical, with the exception of a slight shift to a longer wavelength. The Beer–Lambert law is obeyed across the concentration range from 7×10^{-6} to 1×10^{-4} mol dm^{-3} in $CHCl_3$ in which the absorption spectra were

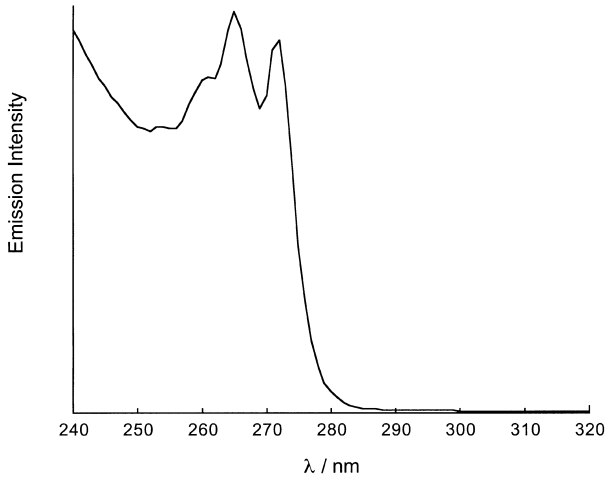

Figure 3. Excitation spectrum of [Dy(tpip)$_3$] in CH_3CN, $\lambda_{em} = 574$ nm.

measured, which confirms the stability of the complexed species. The absorption spectra of the other [Ln(tpip)$_3$] complexes are identical to that shown in Figure 3, confirming that they have the same complex formulation and that the bands observed are characteristic of the tpip ligand. Since deprotonation of the ligand and its subsequent binding to a tripositive metal ion has little effect on the absorption spectrum of the ligand, this is further evidence that the phosphorus-substituted phenyl groups of tpip can be considered as being remote from the imidodiphosphinate binding unit. The value of the ε of the complexes confirms the presence of multiple "remote" benzene harvesting units and precludes the presence of a charge-transfer band in $\lambda >$ 240 nm. This is an advantage for the photophysical studies, because it is well-known that charge-transfer bands present in most of the nitrogen or carboxylate donor sets quench lanthanide luminescence.[9]

The excitation spectrum of [Dy(tpip)$_3$] (Figure 3), monitored at the 574 nm emission band ($^4F_{9/2} \rightarrow {}^6H_{13/2}$), shows a structured band with peaks at 265 and 272 nm. This band closely resembles the absorption spectrum, which demonstrates that the Dy^{3+} emission is sensitised by an energy-transfer process from the tpip ligand. The excitation profile also extends to wavelengths shorter than 250 nm, in agreement with the intense band observed at higher energy in the absorption spectrum of [Eu(tpip)$_3$]. The excitation spectra of [Tb(tpip)$_3$], [Sm(tpip)$_3$] and [Eu(tpip)$_3$] in CH_3CN (monitoring the strongest f–f transition in each case: 545 nm for Tb^{3+} ($^5D_4 \rightarrow {}^7F_5$), 647 nm for Sm^{3+} ($^4G_{5/2} \rightarrow {}^6H_{9/2}$) and 610 nm for Eu^{3+} ($^5D_0 \rightarrow {}^7F_2$)) also confirm that energy transfer takes place from the ligand to the different lanthanides (Supporting Information).

The emission spectrum of a CH_3CN solution of [Eu(tpip)$_3$] is shown in Figure 4. Excitation at 273 nm leads to a strong red emission assigned to the characteristic $^5D_0 \rightarrow {}^7F_J$ ($J = 0-4$) transitions of Eu^{3+}. The dominant band in the corrected emission spectrum is the hypersensitive $^5D_0 \rightarrow {}^7F_2$ transition, which is split into two components (within the resolution of the instrument) that are centred at $\lambda = 610$ and 620 nm. Emission spectra of [Tb(tpip)$_3$], [Sm(tpip)$_3$] and [Dy(tpip)$_3$] complexes (Figure 4) show that the same sensitisation process discussed for [Eu(tpip)$_3$] also occurs in these complexes. Excitation at a wavelength corresponding to ligand-centred

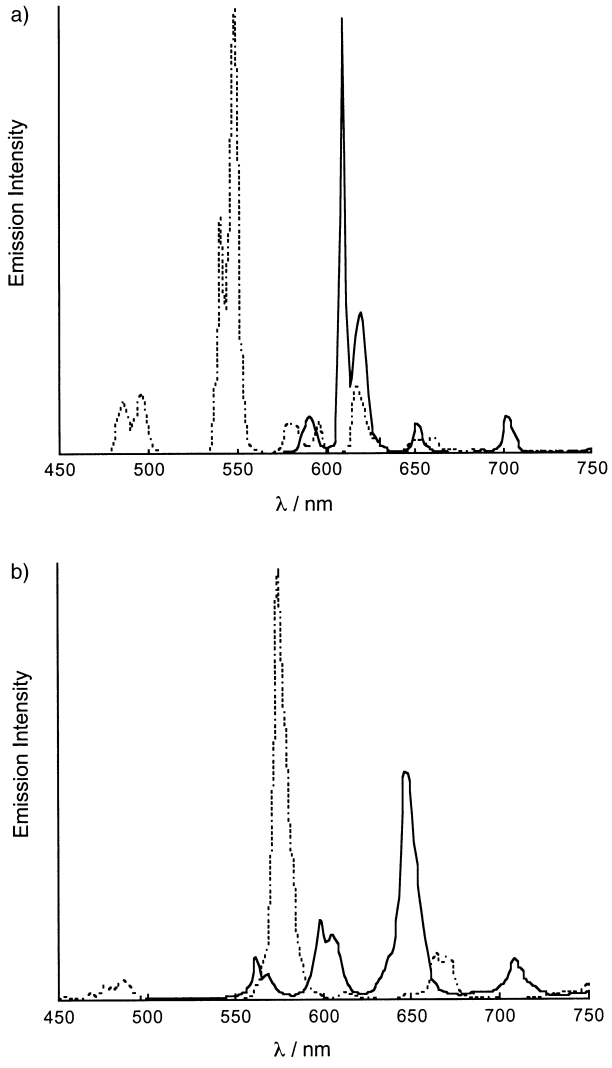

Figure 4. Corrected emission spectra of a) [Eu(tpip)$_3$] (——), [Tb(tpip)$_3$] (••••) (2×10^{-5} mol dm^{-3}), in CH_3CN, $\lambda_{exc} = 273$ nm; b) [Sm(tpip)$_3$] (——), [Dy(tpip)$_3$] (••••) (1×10^{-5} mol dm^{-3}) in CH_3CN, $\lambda_{exc} = 270$ nm, emission intensity not to scale.

  0947-6539/02/0824-5765 $ 20.00+.50/0

bands results in the luminescence characteristic of the Ln^{3+} ion. The emission spectrum of [Tb(tpip)$_3$] shows strong a green emission that is assigned to the $^5D_4 \rightarrow {}^7F_J$ ($J = 2-6$) transitions of Tb^{3+}, with an intense structured $^5D_4 \rightarrow {}^7F_5$ band with peaks at $\lambda = 541$ and 549 nm. Excitation of [Sm(tpip)$_3$] at 270 nm leads to the pink emission of Sm^{3+} assigned to $^4G_{5/2} \rightarrow {}^6H_J$ ($J = 5/2, 7/2, 9/2, 11/2$) transitions; the most intense peak is the hypersensitive transition $^4G_{5/2} \rightarrow {}^6H_{9/2}$ at 647 nm. Similarly, the sensitisation process in [Dy(tpip)$_3$] results in the typical yellow luminescence from Dy^{3+}, with the $^4F_{9/2} \rightarrow {}^6H_J$ ($J = 15/2, 13/2, 11/2$) transitions observable. The latter spectrum is dominated by the hypersensitive $^4F_{9/2} \rightarrow {}^6H_{13/2}$ transition at 575 nm.

In order to further assess the photophysical processes involved in the luminescence of [Ln(tpip)$_3$] (Ln = Eu, Tb, Sm, Dy), the complexes were studied by time-resolved spectroscopy. The measured luminescence lifetimes, following excitation into ligand-centred bands ($\lambda_{exc} = 266$ nm), are displayed in Table 2. All of the luminescence lifetimes measured for these complexes are monoexponential, as expected for one discrete [Ln(tpip)$_3$] solution species.

Table 2. Luminescence lifetimes of the Eu^{3+} ($^5D_0$), Tb^{3+} ($^5D_4$), Sm^{3+} ($^4G_{5/2}$) and Dy^{3+} ($^4F_{9/2}$) levels in [Ln(tpip)$_3$] (Ln = Eu, Tb, Sm, Dy) ($\lambda_{exc} = 266$ nm).

Ln	Conditions[a]	τ [ms]	q
Eu	solid (powder)	2.2	
	dry CH_3CN solution	1.8	
	dry CH_3CN solution + H_2O[b]	0.82	0.7
Tb	solid (powder)	3.1	
	dry CH_3CN solution	2.8	
	dry CH_3CN solution + H_2O[b]	1.4	1.5
Sm	dry CH_3CN solution	0.15	
	dry CH_3CN solution + H_2O[b]	0.06	
Dy	dry CH_3CN solution	0.18	
	dry CH_3CN solution + H_2O[b]	0.12	

[a] Lifetimes measured at room temperature; concentration of CH_3CN solutions = 1×10^{-4} mol dm^{-3}, except for [Dy(tpip)$_3$] with concentration = 1×10^{-5} mol dm^{-3}. [b] [H_2O] = 10 mol dm^{-3}.

The lifetimes of [Eu(tpip)$_3$] and [Tb(tpip)$_3$] in the solid state are 2.2 and 3.1 ms, respectively. These very long lifetimes are characteristic of an absence of deactivating, non-radiative pathways.[23] This is in agreement with the lack of coordinated water molecules we observed in the single-crystal X-ray structures of [Eu(tpip)$_3$] and [Tb(tpip)$_3$]. The tpip ligand was partly chosen because of the absence of any potentially quenching oscillators (e.g. N–H and C–H) in the imidodiphosphinate binding unit, and the measured lifetimes suggest that the role of any other oscillators is minimal. These long lifetimes are in contrast with the short reported values of the [$Eu^{3+} \subset$ 2.2.1] and [$Tb^{3+} \subset$ 2.2.1] cryptates[24] in the solid state, namely 0.31 and 1.5 ms, respectively, which indicate the presence of deactivation pathways from the coordinated water molecules. The results for the tpip complexes compare favourably with the reported luminescence lifetimes (at 298 K) of other solid-state samples that have no coordinated H_2O molecules. For example $[EuCl_2(D_2O)_6]Cl$ and $[TbCl_2(D_2O)_6]Cl$ have lifetimes of 1.64 and 2.38 ms, respectively, while $Na[Eu(EDTA)(D_2O)_3]\cdot 5D_2O$ and $Na[Tb(EDTA)(D_2O)_3]\cdot 5D_2O$ have lifetimes of 1.79 and 2.27 ms, respectively.[23]

In dry acetonitrile, [Eu(tpip)$_3$] and [Tb(tpip)$_3$] also exhibit long-lived luminescence, with lifetimes of 1.8 and 2.8 ms, respectively. These values are only slightly reduced in comparison with the solid-state results, confirming that no water molecules are complexed in the first coordination sphere of the Ln^{3+} ion. The lifetimes of [Sm(tpip)$_3$] and [Dy(tpip)$_3$] in dry CH_3CN are 0.15 and 0.18 ms, respectively. While these are short in comparison with isostructural Eu^{3+} and Tb^{3+} complexes, they are quite long relative to other Sm^{3+} and Dy^{3+} complexes. For comparison, the lifetimes of perchlorate salts of Sm^{3+} and Dy^{3+} in D_2O are reported[25] to be 0.054 and 0.038 ms, while more recently an *m*-terphenyl-based tricarboxylate ligand was used to form 1:1 complexes with Sm^{3+} and Dy^{3+}, with lifetimes in CD_3OD reported to be 0.090 and 0.079 ms, respectively.[26]

The observed lifetimes differ for each Ln^{3+} complex; this can be explained by considering the energy gap between the luminescent state and the highest *J* level of the ground state. This energy gap is similar for Sm^{3+} and Dy^{3+} and amounts to $\approx$7500 and 7800 cm^{-1}, respectively, whereas for Eu^{3+} and Tb^{3+} the gap is larger at 12300 and 14800 cm^{-1}, respectively.[27] For Tb^{3+} and Eu^{3+}, the energy gap is large enough that, to a first approximation, only the high-energy O–H oscillators contribute to vibrational quenching. The smaller gap for Sm^{3+} and Dy^{3+} results in lower frequency vibrations causing significant deactivation. This explains why the lifetimes of the Sm^{3+} and Dy^{3+} complexes are much shorter than those of the Tb^{3+} and Eu^{3+} complexes in dry CH_3CN. Addition of H_2O (10 mol dm^{-3}) to the dry CH_3CN solutions of [Sm(tpip)$_3$] and [Dy(tpip)$_3$] lead to a decrease in the luminescence lifetimes to 0.06 and 0.12 ms, respectively (Table 2). A similar effect was previously observed for the Eu^{III} and Tb^{III} complexes.[12] The observed lifetime reductions correspond to an increase in the decay rate for the complexes of 640 (Eu^{3+}), 350 (Tb^{3+}), $\approx$10000 (Sm^{3+}) and $\approx$2000 s^{-1} (Dy^{3+}). The conformational freedom of the complexes in solution allows the approach and coordination of a water molecule which can lead to such a decrease. The Sm^{3+} and Dy^{3+} luminescence is more efficiently quenched by addition of H_2O than the Eu^{3+} and Tb^{3+} luminescence because the energy gap is bridged by lower vibrational overtones of H_2O. However, the decay rate of Sm^{3+} luminescence increases much more than that of Dy^{3+}, despite the similar energy gap for these two ions. This may be caused by the larger Sm^{3+} ion accommodating an additional deactivating water molecule compared to the Dy^{3+} ion.

An empirical relationship can be used to estimate the number of water molecules coordinated to Eu^{3+} or Tb^{3+} in aqueous solutions.[6] This equation can also be used with CH_3CN as the solvent by measuring the lifetimes following the addition of equal amounts of H_2O or D_2O to the CH_3CN solution.[28] It is possible to estimate the hydration state of the Eu^{3+} and Tb^{3+} ions with Equation (1):

$$q = A(k_{H_2O} - k_{CH_3CN}) \quad (1)$$

Where q is the number of water molecules in the primary coordination sphere, A is a proportionality constant ($A_{Eu} = 1.05$, $A_{Tb} = 4.2$), k_{H_2O} is the observed decay rate in aqueous CH_3CN, k_{CH_3CN} is the observed decay rate in dry CH_3CN. This

0947-6539/02/0824-5766 $ 20.00+.50/0 *Chem. Eur. J.* **2002**, *8*, No. 24

approach has been used successfully with Eu^{3+} and Tb^{3+} complexes of a ligand derived from 1,4,7,10-tetraazacyclododecane.[29] The application of Equation (1) to the values in Table 2 gives $q = 0.71 \pm 0.5$ and 1.5 ± 0.5 for $[Eu(tpip)_3]$ and $[Tb(tpip)_3]$, respectively, in aqueous CH_3CN. This confirms the inner-sphere coordination of water molecules to the Ln^{3+} ion in these complexes. Based on these q values, there is probably one water molecule coordinated to the metal ion of $[Eu(tpip)_3]$ and $[Tb(tpip)_3]$.

In addition to luminescence decay measurements of $[Eu(tpip)_3]$, the growth of the Eu ($^5D_0 \rightarrow {}^7F_2$) luminescence has been examined and found to increase exponentially, with a rise time of 7.5 μs. This initial rise is attributed to the non-radiative decay from the upper $^5D_1$ level to the $^5D_0$ level, from which emission subsequently occurs. The population of the $^5D_1$ level following an energy-transfer process from suitably matched ligand excited states has been noted on numerous occasions. Many europium β-diketonates, for example, have rise times in the region of 2–3 μs, in agreement with the value determined for $[Eu(tpip)_3]$.[30]

Having assessed the factors that control the relative rate of luminescence from the excited Ln^{3+} states, it is important to consider the overall efficiency of the sensitisation process. Luminescence quantum yields were measured for $[Eu(tpip)_3]$ and $[Tb(tpip)_3]$ in dry CH_3CN upon excitation at 273 nm, with $[Ru(bpy)_3]Cl_2$ in aerated H_2O and quinine sulfate in H_2SO_4 (0.5 mol dm^{-3}) as standards. The values obtained are 1.3 % for $[Eu(tpip)_3]$ and 20 % for $[Tb(tpip)_3]$, showing that the overall efficiency of the antenna effect is high.

The quantum yield results were very encouraging as they demonstrate that the tpip ligand can act as a good antenna for both Eu^{3+} and Tb^{3+}, even though no particular attempt was made to select the "remote" energy donors so that there was a good matching of their energy levels with those of the tpip ligand. For many previously reported complexes, sensitisation is only efficient with either Eu^{3+} or Tb^{3+}. For example, the room-temperature quantum yield of $[Eu(acac)_3]$, where acac is the β-diketonate acetylacetonate ligand, is < 0.2 %, whereas the corresponding value for $[Tb(acac)_3]$ is 19 %.[30] Similarly, for the Tb^{3+} complex with *p-t*-butylcalix[4]arene-tetraacetamide, the luminescence quantum yield is 20 % (the same as that measured for $[Tb(tpip)_3]$); however, it is three orders of magnitude lower for the Eu^{3+} complex (0.02 %).[31] In both the acac and the calixarene complexes, the low quantum yield of Eu^{3+} emission was attributed to LMCT deactivation. In contrast, some complexes have a low quantum yield for Tb^{3+} luminescence which arises from an energy back-transfer process occurring from the Tb^{3+} ($^5D_4$) level to a ligand excited state. This is the case for the [Tb ⊂ bpy · bpy · bpy] cryptand; the quantum yield at room temperature is only 3 % in H_2O.[32] This decay process, which is also common for other polypyridine ligands,[1] normally involves energy transfer to the triplet state of the ligand. We measured the phosphorescence of $[Gd(tpip)_3]$ at 77 K to estimate the energy of the triplet state of the tpip ligands in $[Ln(tpip)_3]$. The signal of the phosphorescence band indicates the 0–0 to be ≈ 24 K cm^{-1}. This places the ligand triplet state much higher than the Tb^{III} $^5D_4$ excited state preventing the energy back-transfer process, which reduces the emission efficiency of the Tb^{III} cryptate complexes.

The high quantum yield obtained for $[Tb(tpip)_3]$ complexes can be attributed to a combination of the shielding of the Ln^{3+} ions from quenching solvent molecules (as shown by the lifetime measurements), efficient ligand-to-metal energy transfer and the absence of energy back-transfer. In view of the reasonably high quantum yield and long luminescence lifetime of $[Eu(tpip)_3]$, LMCT states do not appear to play a prominent role in the deactivation of the metal ion. The difference in quantum yield is probably caused by a better match between ligand and metal excited states in $[Tb(tpip)_3]$.

Photophysical studies of lanthanide complexes of Metpip: The absorption spectrum of $[Eu(Metpip)_3]$ in CH_3CN is shown in Figure 5. The measured absorption coefficient is approximately three times greater than that of KMetpip, corresponding to the absorption of three Metpip ligands [λ_{max} [nm] (ε [dm^3 mol^{-1} cm^{-1}]), 278 (6800), 271 (6200)]. Excitation at a wavelength corresponding to ligand-centred bands results in the luminescence characteristic of the Ln^{3+} ion. The excitation spectra of $[Eu(Metpip)_3]$ and

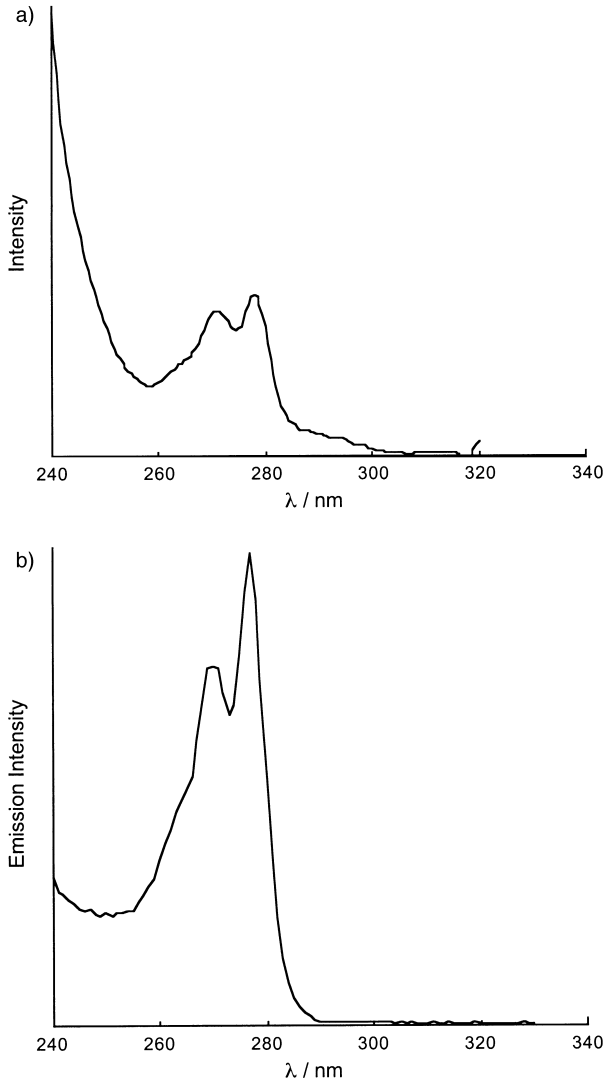

Figure 5. a) Absorption spectrum of $[Eu(Metpip)_3]$ (1×10^{-6} mol dm^{-3}) in CH_3CN. b) Excitation spectrum of $[Eu(Metpip)_3]$ (1×10^{-6} mol dm^{-3}) in CH_3CN; $\lambda_{em} = 610$ nm.

  0947-6539/02/0824-5767 $ 20.00+.50/0

[Tb(Metpip)$_3$] solutions show one structured band with peaks at 270 and 277 nm (Figure 5). bThis band matches the vibronic band observed for the *o*-tolyl groups in the absorption spectrum of [Eu(Metpip)$_3$]. This demonstrates that the sensitisation process which occurs in [Ln(tpip)$_3$] (Ln = Sm, Eu, Tb, Dy) complexes also operates in [Eu(Metpip)$_3$] and [Tb(Metpip)$_3$].

Steady-state luminescence spectra of CH_3CN solutions of [Eu(Metpip)$_3$] and [Tb(Metpip)$_3$] are shown in Figure 6. For [Eu(Metpip)$_3$], the characteristic $^5D_0 \rightarrow {}^7F_J$ ($J = 0-4$) transitions of Eu^{3+} are observed in the emission spectrum, with the

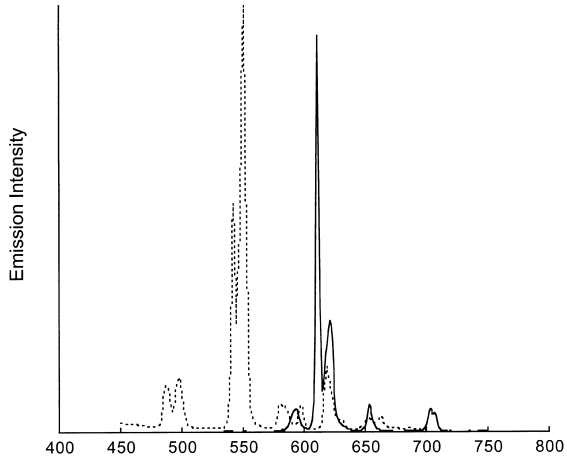

Figure 6. Corrected emission spectra of [Eu(Metpip)$_3$] (——) and [Tb(Metpip)$_3$] (••••) in CH_3CN, $\lambda_{em} = 610$ nm and 550 nm, respectively; $\lambda_{exc} = 273$ nm, emission intensity not to scale.

hypersensitive $^5D_0 \rightarrow {}^7F_2$ transition resolved into two components centred on 611 and 621 nm. The $^5D_4 \rightarrow {}^7F_J$ ($J = 2-6$) transitions of Tb^{3+} are observed for [Tb(Metpip)$_3$], with an intense structured $^5D_4 \rightarrow {}^7F_5$ band that has peaks at 542 and 551 nm. In terms of the splitting and relative intensities of the f–f transitions, the emission spectra of [Eu(Metpip)$_3$] and [Tb(Metpip)$_3$] are almost identical to the spectra recorded for their respective tpip analogues, indicative of a high degree of structural similarity between [Ln(tpip)$_3$] and [Ln(Metpip)$_3$] complexes in solution.

In order to investigate the possibility of solvent coordination in solution, time-resolved luminescence spectroscopy has been performed on [Eu(Metpip)$_3$] and [Tb(Metpip)$_3$] in both the solid state and in solution. The measured luminescence lifetimes, following excitation into ligand-centred bands ($\lambda_{exc} = 266$ nm), are displayed in Table 3. All of the decays are monoexponential.

The measured lifetimes at room temperature of [Eu(Metpip)$_3$] and [Tb(Metpip)$_3$] as powdered solids appear to be rather short in comparison with the analogous tpip complexes. The increase in decay rate for [Eu(Metpip)$_3$] compared with [Eu(tpip)$_3$] is 550 s^{-1}; the increase for [Tb(Metpip)$_3$] compared with [Tb(tpip)$_3$] is 390 s^{-1}. However, the crystal structure of [Eu(Metpip)$_3$], elemental analyses and IR spectroscopy give no evidence of solvent content in [Ln(Metpip)$_3$] (Ln = Eu and Tb) in the solid state. This significant increase in the decay rate is attributed to the presence of a new deactivating pathway. A temperature-dependent pathway can be eliminated, as the solid-state luminescence lifetimes do not change upon lowering the temperature to 77 K (Table 3). This implies that the higher decay rate is not caused by energy back-transfer to ligand excited states or to a charge-transfer mechanism. The increase in decay rate for [Ln(Metpip)$_3$] could be associated with vibrational deactivation, and in the absence of coordinated solvent molecules such deactivation would be caused by the ligand itself. We attribute the increase in the luminescence decay rate to the presence of an additional 36 C–H oscillators in the Metpip complexes compared to those of tpip. Although C–H vibrations are much less efficient in quenching the luminescence than O–H vibrations, the cumulative effect can be large. In the Eu^{3+} complex of a substituted 1,4,7,10-tetraazacyclododecane, for example, the average contribution of each C–H oscillator to the decay rate was either 5 s^{-1} or 26 s^{-1} depending on the distance between the oscillator and the Ln^{3+} ion.[33] Studies of other lanthanide complexes have produced similar estimates.[34]

Table 3. Luminescence lifetimes of the Eu^{3+} ($^5D_0$) and Tb^{3+} ($^5D_4$) levels in [Ln(Metpip)$_3$] (Ln = Eu, Tb) ($\lambda_{exc} = 266$ nm).

Ln	Conditions[a]	τ [ms]	q
Eu	solid (powder, RT)	1.0	
	solid (powder, 77 K)	0.99	
	dry CH_3CN solution	1.3	
	dry CH_3CN solution + H_2O[b]	1.1	0.14
Tb	solid (powder, RT)	1.4	
	solid (powder, 77 K)	1.4	
	dry CH_3CN solution	1.9	
	dry CH_3CN solution + H_2O[b]	1.7	0.29

[a] Solution lifetimes measured at room temperature; concentration of CH_3CN solutions = 1×10^{-6} mol dm^{-3}; [b] [H_2O] = 10 mol dm^{-3}.

In dry CH_3CN, the lifetimes of the Eu^{3+} ($^5D_0$) level in [Eu(Metpip)$_3$] and the Tb^{3+} ($^5D_4$) level in [Tb(Metpip)$_3$] increase to 1.33 and 1.89 ms, respectively. A longer lifetime in solution compared with the solid state is not uncommon and is good evidence that solvent molecules are not deactivating the excited state. For example, nine-coordinate complexes of Eu^{3+} with tripodal ligands, in which there are no coordinated water molecules, have shorter lifetimes in the solid state than in dry CH_3CN.[28]

Upon addition of H_2O (10 mol dm^{-3}) to these anhydrous solutions, there is a slight reduction in the lifetimes of both the Eu^{3+} ($^5D_0$) and the Tb^{3+} ($^5D_4$) lifetimes to 1.13 and 1.67 ms, respectively. This reduction upon adding water is much smaller than that observed with [Eu(tpip)$_3$] and [Tb(tpip)$_3$] (in spite of the 100-fold increase in the H_2O:complex ratio for [Ln(Metpip)$_3$] compared with [Ln(tpip)$_3$]), and is consistent with H_2O molecules solely interacting in the second coordination sphere of the Ln^{3+} ion.

Application of Equation (1) to the values in Table 3 gives $q = 0.14$ and 0.29 for [Eu(Metpip)$_3$] and [Tb(Metpip)$_3$] in aqueous CH_3CN, which supports the conclusion that there are no water molecules coordinated to the lanthanide ion and the minor quenching is attributed to second-sphere interactions in contrast with [Ln(tpip)$_3$] in aqueous CH_3CN. This change to outer-sphere coordination is attributed to the greater shielding of the Ln^{3+} ion by the bulky *o*-tolyl groups in the Metpip ligand.

0947-6539/02/0824-5768 $ 20.00+.50/0 *Chem. Eur. J.* **2002**, *8*, No. 24

Conclusion

In this paper we demonstrate that the assembly of tetraaryl imidodiphosphinates ligands around lanthanide ions leads to complexes with efficient lanthanide luminescence sensitisation for all lanthanides emitting in the visible region, namely, Eu^{III}, Tb^{III}, Dy^{III} and Sm^{III}. This is attributed to several factors incorporated in the ligand design: i) shielding of the ion from the water molecules by encapsulation with the three-ligand structure to form a hydrophobic shell around the ion; ii) the flexibility of the design to allow an extra "built-in" shield on the ligand which blocks the approach of water molecules; iii) the lack of any strong ligand-to-metal charge-transfer bands that are usually responsible for the weak emission of the more readily reduced lanthanides; iv) the lack of any energy back-transfer from the sensitiser triplet state. Although the exclusion of coordinating solvent molecules by structurally complex polydentate ligands is not uncommon, the same result which is achieved with only three bidentate ligands is very unusual and suggests that this assembly approach could be extended to other simple ligand systems.

It is the flexibility of imidodiphosphinates that makes them most useful as antenna ligands, since they offer a wealth of possibilities for further derivitisation. Since the binding and antenna domains are not in conjugation, imidodiphosphinate complexes can be altered whilst maintaining binding properties. Simply exchanging one Ln^{3+} ion for another allows the complex to be tuned so that light emission is centred on four different wavelengths, with no attendant changes to structure or absorption wavelength. It should be possible to further modify the ligands to optimise the antenna groups for a particular Ln^{3+} ion, and to incorporate new physical properties (e.g. solubility) as required.

The aforementioned properties of the ligands are particularly important in the search for new luminescent lanthanide complexes for application as photonic devices and sensors. Neutral lanthanide complexes are also highly desired for applications in biological systems to minimise possible non-specific binding. Further studies in our group into the development of lanthanide imidodiphosphinate complexes are underway.

Experimental Section

Equipment: ^{1}H, ^{13}C{^{1}H} and ^{31}P{^{1}H} NMR spectra were recorded on Bruker AC-200, 250 and 360 MHz spectrometers. ^{1}H and ^{13}C{^{1}H} shifts were referenced to external $SiMe_4$, while ^{31}P{^{1}H} shifts were referenced to external 85% aqueous phosphoric acid. Positive-ion FAB mass spectra were recorded on a Kratos MS-50 mass spectrometer in a *m*-nitrobenzyl alcohol matrix. Elemental analyses were performed on a Perkin-Elmer 2400 CHN elemental analyser. IR spectra were obtained from KBr pellets with a Perkin–Elmer 1710 Fourier Transform spectrometer. UV/Vis absorption spectra were recorded on a Perkin–Elmer Lambda 9 spectrometer. All measurements were made at room temperature (≈20 °C) in aerated solutions, unless otherwise stated.

Luminescence emission and excitation spectra were recorded on a Photon Technology International (PTI) QM-1 emission spectrometer, previously described.[35] Emission spectra were typically obtained with an excitation and emission band-pass of 5 nm, with the most highly resolved spectra having an emission band-pass of 1 nm. Emission spectra were corrected for the wavelength dependence of the PMT. Uncorrected excitation spectra were typically obtained with an excitation and emission band-pass of 5 nm, with the most highly resolved spectra having an excitation band-pass of 1 nm. Lifetime measurements were carried out with a nanosecond Nd-YAG laser (Continuum, Surelite II) as the excitation source. The fourth harmonic output of the laser was used for excitation at 266 nm. Emission from the sample was collected at 90°, passed through appropriate cut-off filters and detected by a photomultiplier tube (Hamamatsu R928) following wavelength selection by a PC-controlled monochromator (PTI model 101) with a band-pass of 5 nm. In the excitation spectra, the emission was monitored at 616 nm for Eu^{3+} ($^5D_0$), 545 nm for Tb^{3+} ($^5D_4$), 647 nm for Sm^{3+} ($^4G_{5/2}$) and 574 nm for Dy^{3+} ($^4F_{9/2}$). The signal from the photomultiplier tube was processed through a digital storage oscilloscope (LeCroy 9350 AM, 500 MHz), triggered by the laser pulse. For room temperature measurements, solution samples were placed in 1 cm quartz cuvette and powdered solid samples in a quartz tube. For measurements at 77 K, samples were placed in a quartz tube and cooled in a quartz Dewar filled with liquid nitrogen.

Data analysis: The emission decay curves were averaged over 1000 laser shots and transferred to a PC for analysis. The so-obtained unweighted data were analysed by a non-linear least-squares iterative technique (Marquardt–Levenberg algorithm) by means of the Kaleidagraph software. The luminescence decay curves were fitted to a single exponential of the form $I(t) = I(0)\exp(-t/\tau)$, where $I(t)$ is the intensity at time t after the excitation flash, $I(0)$ is the initial intensity at $t = 0$ and τ is the luminescence lifetime. High Pearson's correlation coefficients (≥ 0.999) were observed in all cases. Lifetimes were reproducible to ±5%.

Luminescence quantum yields were measured by an optically dilute relative method[36] with $[Ru(2,2'\text{-bipyridyl})_3]Cl_2$ ($\Phi = 0.028$ in aerated H_2O)[37] and quinine sulfate ($\Phi = 0.546$ in aerated H_2SO_4 (0.5 mol dm^{-3})[38] as standards for complexes of europium(III) and terbium(III), respectively. Europium(III) emission was measured between $\lambda = 550$ and 750 nm, corresponding to the dominant $^5D_0 \rightarrow {}^7F_J$ ($J = 0-4$) transitions, while terbium(III) emission was measured between $\lambda = 450$ nm and 700 nm, corresponding to the $^5D_4 \rightarrow {}^7F_J$ ($J = 0-6$) transitions. The accuracy of these procedures is estimated to be ±10%.

Materials: Starting materials were of reagent grade, obtained from Aldrich or Acros, and used without further purification, unless otherwise stated. Lanthanide(III) chlorides were obtained from Aldrich or Acros (99.9%) and used as received. Deuterated solvents were obtained from Goss Scientific and used as received. Anhydrous solvents, when required, were freshly distilled over the appropriate drying agents under dinitrogen. Reactions requiring anhydrous conditions were performed under dinitrogen by means of standard Schlenck and vacuum-line techniques

For the photophysical studies, DMF and methanol were of spectroscopic grade and used as received. CH_3CN was dried over P_2O_5 (5% *w*/*v*) and freshly distilled prior to use. Water was purified by a Millipore (Milli-RO 15) water purification system.

Htpip:[13] A solution of chlorodiphenylphosphine (4.07 g, 18.4 mmol) and hexamethyldisilazane (1.49 g, 9.23 mmol) in toluene (30 mL) was refluxed for 3 h, after which time Me_3SiCl was distilled off. The mixture was cooled for 10 minutes in an ice bath and a solution of H_2O_2 (2 mL, 27.5 wt.% in H_2O) in THF (4 mL) was added dropwise. This solution was added to diethyl ether (50 mL) resulting in the formation of a white precipitate. This solid was washed several times with water and recrystallised from methanol to give the desired product (1.0 g, 26%). ^{1}H NMR (200 MHz, $CDCl_3$): $\delta =$ 7.48–7.27 (m, 12H; Ar), 7.80–7.65 (m, 8H; Ar); ^{31}P{^{1}H} NMR (101 MHz, $CDCl_3$): $\delta = 21.0$ (s); FAB-MS: m/z: 418 $[M+H]^+$, 219 $[M - Ph_2PO+2H]^+$; UV/Vis (EtOH): λ_{max} (ε [dm^3 mol^{-1} cm^{-1}]) = 261 (2060), 266 (2460), 273 (1940) nm.

Chlorodi-2-methylphenylphosphine:[17] A solution of *o*-bromotoluene (10.0 g, 57.9 mmol) in dry THF (10 mL) was added dropwise under nitrogen to dry magnesium turnings (1.57 g, 64.6 mmol). The reaction mixture was stirred for 1 h, after which time formation of the Grignard reagent was complete. The Grignard reagent, and washings in dry THF (7 mL), were added dropwise to a solution of phosphorus trichloride (2.2 mL, 25 mmol) in dry THF (10 mL) cooled in an ice bath. After a few minutes, a large amount of white precipitate formed. This mixture was stirred at room temperature for 23 h, filtered and washed with dry toluene (20 cm^3). The solvent was removed from a small sample of this solution, and

  0947-6539/02/0824-5769 $ 20.00+.50/0

the resultant material was identified as the desired compound by ^{1}H and ^{31}P NMR spectroscopy. Because of the sensitivity of the material, the THF/toluene solution of this compound was used without further purification. ^{1}H NMR (250 MHz, $CDCl_3$): $\delta = 2.47$ (d, 6H, $^4J(P,H) = 2.7$ Hz, CH_3); $^{31}P\{^1H\}$ NMR (101 MHz, $CDCl_3$): $\delta = 74.4$ (s).

***N*-(*P*,*P*-Di-2-methylphenylphosphinoyl)-*P*,*P*-di-2-methylphenyl-phosphinimidic acid (Metpip)**: Hexamethyldisilazane (1.59 g, 9.85 mmol) was dissolved in dry toluene (2 mL) and added dropwise to a solution of chlorodi-2-methylphenylphosphine in toluene/THF under nitrogen (25 mmol, assuming 100% yield of preparation described above). This solution was refluxed for 4.5 h, after which time Me_3SiCl and THF were distilled off. The solution was cooled in an ice bath for 30 minutes. H_2O_2 (1.7 mL, 35 wt.% in H_2O) in THF (2 mL) was added dropwise, and the solution stirred for 18 h. This solution was added to diethyl ether (50 mL), resulting in the immediate precipitation of a white solid. The solid was filtered and washed with water and MeOH to give the desired product (0.71 g, 15%, based on hexamethyldisilazane). ^{1}H NMR (250 MHz, $CDCl_3$): $\delta = 7.82-7.74$ (m, 4H; Ar), 7.33–7.27 (m, 4H; Ar), 7.14–7.00 (m, 8H; Ar), 2.18 (s, 12H; CH_3); $^{31}P\{^1H\}$ NMR (101 MHz, $CDCl_3$): $\delta = 25.4$ (s); IR (KBr): $\tilde{\nu} = 1196$, 1215 and 1229 (PNP) and 1068, 1094 cm^{-1} (PO); FAB-MS: m/z: 474 $[M+H]^+$; elemental analysis calcd (%) for $C_{28}H_{29}NO_2P_2 \cdot 0.5\,H_2O$: C 69.70, H 6.27, N 2.90; found: C 69.89, H 6.10, N 2.77.

Potassium tetraphenylimidodiphosphinate (Ktpip): Htpip (0.30 g, 0.72 mmol) was dissolved in a 2% methanolic KOH solution (10 mL). The solvent volume was decreased to 2 mL under reduced pressure and diethyl ether was added (20 mL). The resultant solid was recrystallised from ethanol to give the desired product (0.187 g, 58%). ^{1}H NMR (360 MHz, D_2O): $\delta = 7.79-7.73$ (m, 8H; Ar), 7.52–7.41 (m, 12H; Ar); $^{31}P\{^1H\}$ NMR (146 MHz, D_2O): $\delta = 17.0$ (s); FAB-MS: m/z: 456 $[M+H]^+$.

KMetpip: Metpip (0.615 g, 1.30 mmol) was heated at reflux for 1 h in a 10% methanolic KOH solution (30 mL). The solvent was removed under reduced pressure and the resultant white solid was washed with water (5 mL). This solid was recrystallised from ethanol to give the desired product (0.390 g, 59%). Single crystals of KMetpip suitable for an X-ray diffraction analysis were grown by slow evaporation from a methanolic solution. ^{1}H NMR (200 MHz, CD_3OD): $\delta = 8.31-8.20$ ((m, 4H; Ar), 7.29–6.99 (m, 12H; Ar), 2.12 (s, 12H; CH_3); $^{31}P\{^1H\}$ NMR (81 MHz, CD_3OD): $\delta = 9.1$ (s); FAB-MS: m/z: 512 $[M+H]^+$, 550 $[M+K]^+$; UV/Vis (MeOH): λ_{max} (ε [dm^{3}mol^{-1}cm^{-1}]) = 270 (2700), 277 nm (2500); elemental analysis calcd (%) for $C_{28}H_{28}KNO_2P_2 \cdot 3.5\,H_2O$: C 58.53, H 6.14, N 2.44; found: C 58.19, H 6.30, N 2.25.

Ln(tpip)$_3$ (Ln = Eu, Tb, Sm, Dy): To a solution of Ktpip (3 equiv, 0.187 g, 0.41 mmol) in H_2O, was added dropwise $LnCl_3 \cdot x\,H_2O$ (1 equiv) dissolved in H_2O. The white solid that immediately precipitated was filtered, washed with H_2O several times and dried under vacuum to give the corresponding [Ln(tpip)$_3$] in 70–80% yield.

[Eu(tpip)$_3$]: ^{1}H NMR (360 MHz, $CDCl_3$): $\delta = 7.54-7.48$ (m, 24H; Ar), 7.21 (t, 12H; $^3J(H,H) = 7.4$ Hz, Ar), 6.95–6.99 (m, 24H; Ar); $^{13}C\{^1H\}$ NMR (91 MHz, $CDCl_3$): $\delta = 129.8$ (d, $^1J(P,C) = 137$ Hz, quart. C), 129.4 (s), 128.9 (d, $J(P,C) = 10$ Hz), 127.0 (d, $J(P,C) = 13$ Hz); $^{31}P\{^1H\}$ NMR (146 MHz, $CDCl_3$): $\delta = 37.7$ (s); FAB-MS: m/z: 1400 $[M+H]^+$, 983 $[M-tpip]^+$; UV/Vis ($CHCl_3$): λ_{max} (ε [dm^{3}mol^{-1}cm^{-1}]) = 273 nm (5000); elemental analysis calcd (%) for $C_{72}H_{60}EuN_3O_6 \cdot 3\,H_2O$: C 59.43, H 4.57, N 2.89; found: C 59.16, H 4.24, N 2.83.

[Tb(tpip)$_3$]: ^{1}H NMR (360 MHz, $CDCl_3$): $\delta = 7.97$ (brs, 24H; Ar), 7.35 (s, 12H; *p*-Ar), 6.28 (s, 24H; Ar); $^{13}C\{^1H\}$ NMR (91 MHz, $CDCl_3$): $\delta = 159.3$ (quart. C), 134.5 (s), 130.4 (s), 128.6 (s); $^{31}P\{^1H\}$ NMR (146 MHz, $CDCl_3$): $\delta = 200.7$ (s); FAB-MS: m/z: 1408 $[M+H]^+$, 991 $[M-tpip]^+$.

[Sm(tpip)$_3$]: ^{1}H NMR (250 MHz, $CDCl_3$): $\delta = 7.66-7.58$ (m, 24H; Ar), 7.26–7.19 (m, 12H; *p*-Ar), 7.08–7.03 (m, 12H; Ar); $^{13}C\{^1H\}$ NMR (63 MHz, $CDCl_3$): $\delta = 131.1$, 131.0, 130.9, 129.8, 127.5, 127.4, 127.3 [s, d, d, d]; $^{31}P\{^1H\}$ NMR (101 MHz, $CDCl_3$) 25.1 (s); FAB-MS: m/z: 1403 $[M+H]^+$, 985 $[M-tpip]^+$.

[Dy(tpip)$_3$]: ^{1}H NMR (250 MHz, $CDCl_3$): $\delta = 8.1$ (brs, 24H; Ar), 7.45 (brs, 12H; *p*-Ar), 6.57 (brs, 24H; Ar); $^{13}C\{^1H\}$ NMR (63 MHz, $CDCl_3$): $\delta = 154$ (brs), 132.6 (s), 130.2 (s), 128.3 (s); $^{31}P\{^1H\}$ NMR (101 MHz, $CDCl_3$): $\delta =$ 147.9 (s); FAB-MS: m/z: 1414 $[M+H]^+$, 997 $[M-tpip]^+$.

[Eu(Metpip)$_3$]: $EuCl_3 \cdot 6\,H_2O$ (0.016 g, 0.044 mmol) dissolved in methanol (1 mL) was added dropwise to a solution of KMetpip (0.067 g, 0.13 mmol) in methanol (5 mL). The white solid that immediately precipitated was filtered, washed with methanol (2×2 mL) and dried under vacuum (0.054 g, 78%). Single crystals, suitable for an X-ray diffraction analysis, were grown by slow evaporation from a $CHCl_3$ solution. ^{1}H NMR (250 MHz, $CDCl_3$): $\delta = 7.16-7.15$ (m, 24H; Ar), 6.31–6.10 (m, 24H; Ar), 3.06 (s, 36H; CH_3); $^{31}P\{^1H\}$ NMR (101 MHz, $CDCl_3$): $\delta = 25.7$ (s); IR (KBr): $\tilde{\nu} = 1224$, 1195 (PNP) and 1098, 1071 cm^{-1} (PO); FAB-MS: m/z: 1571 $[M+H]^+$, 1097 $[M-Metpip]^+$; UV/Vis (CH_3CN): λ_{max} (ε [dm^{3}mol^{-1}cm^{-1}]) = 278 (6800), 271 nm (6200); elemental analysis calcd (%) for $C_{84}H_{84}EuN_3O_6P_6$: C 64.29, H 5.39, N 2.68; found: C 63.95, H 5.55, N 2.52.

[Tb(Metpip)$_3$]: $TbCl_3 \cdot 6\,H_2O$ (0.014 g, 0.037 mmol) dissolved in methanol (1 mL) was added dropwise to a solution of KMetpip (0.053 g, 0.10 mmol) in methanol (8 mL). The white solid that immediately precipitated was filtered, washed with methanol (2×2 mL) and dried under vacuum (0.050 g, 86%). $^{31}P\{^1H\}$ NMR (101 MHz, $CDCl_3$): $\delta = 142$ (brs); IR (KBr): $\tilde{\nu} = 1224$, 1195 (PNP) and 1098, 1071 cm^{-1} (PO); FAB-MS: m/z: 1576 $[M+H]^+$, 1103 $[M-Metpip]^+$; elemental analysis calcd (%) for $C_{84}H_{84}TbN_3O_6P_6$: C 64.00, H 5.37, N 2.67; found: C 63.62, H 5.47, N 2.57.

Crystal structure analysis: Single-crystal X-ray diffraction data were collected on a Stoe Stadi-4 diffractometer equipped with an Oxford Cryosystems low-temperature device operating at 220 K. $Cu_{K\alpha}$ radiation was used for the potassium complex, and the structure was solved by direct methods (SIR 92).[39] $Mo_{K\alpha}$ radiation was used for the Eu complex, and its structure was solved by Patterson methods (DIRDIF).[40] Absorption corrections based on ψ scans were applied to both data sets. Both structures were refined by full-matrix least-squares against F^2 (Shelxtl),[41] with H atoms in idealised positions. Further analysis was performed with Platon.[42]

Crystallographic data of [K(Metpip)(MeOH)$_2$(H$_2$O)]$_n$: $C_{30}H_{38}KNO_5P_2$, $M = 593.65$, orthorhombic, space group $Pna2_1$, $a = 16.956(7)$, $b = 22.495(5)$, $c = 8.0303(19)$ Å, $V = 3063.0(16)$ Å^3, $Z = 4$, $\rho_{calcd} = 1.287$ g cm^{-3}, $F(000) = 1256$, $\mu = 2.817$ mm^{-1}, $R_1 = 0.0709$ [$\theta_{max} = 70°$, 1556 data $F > 4\sigma(F)$], $wR_2 = 0.1716$ for 2854 independent reflections, GOF = 0.977.

Crystallographic data of [Eu(Metpip)$_3$]·CHCl$_3$: Single crystals of [Eu(Metpip)$_3$], suitable for X-ray diffraction analysis, were grown by slow evaporation from a $CHCl_3$ solution. $C_{85}H_{85}Cl_3EuN_3O_6P_6$, $M = 1688.69$, rhombohedral, space group $R\bar{3}$, $a = b = 15.2788(6)$, $c = 30.532(5)$ Å, $V = 6172.5(10)$ Å^3, $Z = 3$, $\rho_{calcd} = 1.363$ g cm^{-3}, $F(000) = 2604$, $\mu = 1.029$ mm^{-1}, $R_1 = 0.0549$ [$\theta_{max} = 25°$, 2217 data $F > 4\sigma(F)$], $wR = 0.1296$ for 2418 independent reflections, GOF = 1.113. The point group of this complex is 3; however, it is disordered about at crystallographic -3 special position. Similarity and rigid bond restraints were applied to all light-atom anisotropic displacement parameters. The chloroform of solvation was also disordered, its geometry was controlled during refinement by the application of explicit restraints.

CCDC-187661 and -187662 contain the supplementary crystallographic data for this paper. These data can be obtained free of charge via www.ccdc.cam.ac.uk/conts/retrieving.html (or from the Cambridge Crystallographic Data Centre, 12 Union Road, Cambridge CB2 1EZ, UK; fax: (+44) 1223-336033; or deposit@ccdc.cam.uk).

Acknowledgement

Support for this work from EPSRC (S.W.M) is gratefully acknowledged. The authors gratefully acknowledge the assistance of Ross Blackwood in preparing the [Sm(tpip)$_3$] and [Dy(tpip)$_3$] samples.

[1] N. Sabbatini, M. Guardigli, J. M. Lehn, *Coord. Chem. Rev.* **1993**, *123*, 201.

[2] T. Jüstel, H. Nikol, C. Ronda, *Angew. Chem.* **1998**, *110*, 3250; *Angew. Chem. Int. Ed.* **1998**, *37*, 3084; C. M. Rudzinski, A. M. Young, D. G. Nocera, *J. Am. Chem. Soc.* **2002**, *124*, 1723; M. P. Lowe, D. Parker, O. Reany, S. Aime, M. Botta, G. Castellano, E. Gianolio, R. Pagliarin, *J. Am. Chem. Soc.* **2001**, *123*, 7601; L. Charbonniere, R. Ziessel, M. Guardigli, A. Roda, N. Sabbatini, M. Cesario, *J. Am. Chem. Soc.* **2001**, *123*, 2436; K. Kuriki, Y. Koitke, Y. Okamoto, *Chem. Rev.* **2002**, *102*, 2347.

[3] P. Gawryszewska, L. Jerzykiewicz, M. Pietraszkiewicz, J. Legendziewicz, J. P. Riehl, *Inorg. Chem.* **2000**, *39*, 5365.

  0947-6539/02/0824-5770 $ 20.00+.50/0 *Chem. Eur. J.* **2002**, *8*, No. 24

[4] E. B. van der Tol, H. J. van Ramesdonk, J. W. Verhoeven, F. J. Steemers, E. G. Kerver, W. Verboom, D. N. Reinhoudt, *Chem. Eur. J.* **1998**, *4*, 2315; G. Ulrich, R. Ziessel, I. Manet, M. Guardigli, N. Sabbatini, F. Fraternali, G. Wipff, *Chem. Eur. J.* **1997**, *3*, 1815; C. Fischer, G. Sarti, A. Casnati, B. Carrettoni, I. Manet, R. Schuurman, M. Guardigli, N. Sabbatini, R. Ungaro, *Chem. Eur. J.* **2000**, *6*, 1026.
[5] G. R. Motson, O. Mamula, J. C. Jeffery, J. A. McCleverty, M. D. Ward, A. von Zelewsky, *J. Chem. Soc. Dalton Trans.* **2001**, 1389; M. P. Lowe, P. Caravan, S. J. Rettig, C. Orvig, *Inorg. Chem.* **1998**, *37*, 1637; G. Ulrich, M. Hissler, R. Ziessel, I. Manet, G. Sarti, N. Sabbatini, *New J. Chem.* **1997**, *21*, 147; N. Armaroli, G. Accorsi, P. Barigelletti, S. M. Couchman, J. S. Fleming, N. C. Harden, J. C. Jeffery, K. L. V. Mann, J. A. McCleverty, L. H. Rees, S. R. Starling, M. D. Ward, *Inorg. Chem.* **1999**, *38*, 5769; Y. Bretonnière, R. Wietzke, C. Lebrun, M. Mazzanti, J. Pécaut, *Inorg. Chem.* **2000**, *39*, 3499; J. J. Lessmann, W. J. DeW. Horrocks, *Inorg. Chem.* **2000**, *39*, 3114.
[6] W. DeW. Horrocks, Jr., D. R. Sudnick, *Acc. Chem. Res.* **1981**, *14*, 384.
[7] C. Piguet, J. C. G. Bunzli, *Chem. Soc. Rev.* **1999**, *28*, 347.
[8] S. Aime, M. Botta, R. S. Dickins, C. L. Maupin, D. Parker, J. P. Riehl, J. A. G. Williams, *J. Chem. Soc. Dalton Trans.* **1998**, 881; P. R. Selvin, J. Jancarik, M. Li, L.-W. Hung, *Inorg. Chem.* **1996**, *35*, 700; N. Sato, S. Shinkai, *J. Chem. Soc. Perkin Trans. 2* **1993**, 621; Z. Pikramenou, J. A. Yu, R. B. Lessard, A. Ponce, P. A. Wong, D. G. Nocera, *Coord. Chem. Rev.* **1994**, *132*, 181.
[9] M. A. Mortellaro, D. G. Nocera, *J. Am. Chem. Soc.* **1996**, *118*, 7414.
[10] W. J. DeW. Horrocks, M. Albin, in *Progr. Inorg. Chem.*, *Vol. 31* (Ed.: S. J. Lippard), Wiley, New York, **1984**, p. 1.
[11] J. Yuan, K. Matsumoto, *Anal. Sci.* **1996**, *12*, 31; C. M. Deary, R. M. Dysan, T. W. Hambley, M. Lawreance, M. Maeder, G. A. Tannock, *Aust. J. Chem. Soc.* **1993**, *46*, 577.
[12] S. W. Magennis, S. Parsons, A. Corval, J. D. Woollins, Z. Pikramenou, *Chem. Commun.* **1999**, 61.
[13] D. J. Williams, *Inorg. Nucl. Chem. Lett.* **1980**, *16*, 189.
[14] H. Nöth, *Z. Naturforsch. B* **1982**, *37*, 1491.
[15] D. J. Williams, I. Fleming, *Spectroscopic Methods in Organic Chemistry*, *Vol. Ch. 1*, 5th ed., McGraw-Hill, London, **1995**.
[16] K. L. Paciorek, *Inorg. Chem.* **1964**, *3*, 96.
[17] P. W. Clark, B. J. Mulraney, *J. Organomet. Chem.* **1981**, *217*, 51.
[18] I. Rodríguez, C. Alvarez, J. Gómez-Lara, R. Cea-Olivares, *Lanthan. Actin. Res.* **1986**, *1*, 253.
[19] J. Reuben, *Progr. NMR Spectrosc.* **1975**, *9*, 1.
[20] R. O. Day, R. R. Holmes, A. Schmidpeter, K. Stoll, L. Howe, *Chem. Ber.* **1991**, *124*, 2443.
[21] A. O. Gudima, E. O. Berezhnoi, V. A. Kalibabchuk, *Koord. Khim.* **1990**, *16*, 1147.
[22] A. D. Sherry, C. F. G. C. Geraldes, *Spectroscopic Methods in Organic Chemistry*, *Ch. 4* (Eds.: J.-C. G. Bünzli, G. R. Chopin), Elsevier, Amsterdam, **1989**.
[23] J.-C. G. Bünzli, *Spectroscopic Methods in Organic Chemistry*, *Ch. 7* (Eds.: J.-C. G. Bünzli, G. R. Chopin), Elsevier, Amsterdam, **1989**.
[24] N. Sabbatini, S. Dellonte, G. Blasse, *Chem. Phys. Lett.* **1986**, *129*, 541; N. Sabbatini, M. Ciano, S. Dellonte, A. Bonazzi, F. Bolletta, V. Balzani, *J. Phys. Chem.* **1984**, *88*, 1534.
[25] G. Stein, E. Würzberg, *J. Chem. Phys.* **1975**, *62*, 208.
[26] M. P. O. Wolbers, F. van Veggel, B. H. M. Snellink-Ruel, J. W. Hofstraat, F. A. J. Geurts, D. N. Reinhoudt, *J. Chem. Soc. Perkin Trans. 2* **1998**, 2141.
[27] W. T. Carnall, *Spectroscopic Methods in Organic Chemistry*, *Vol. 3*, (Eds.: K. A. J. Gschneidner, L. Eyring), North Holland, Amsterdam, **1979**, Chapter 24.
[28] F. Renaud, C. Piguet, G. Bernardinelli, J.-C. Bünzli, G. Hopfgartner, *J. Am. Chem. Soc.* **1999**, *121*, 9326.
[29] G. Zucchi, R. Scopelliti, P.-A. Pittet, J.-C. G. Bünzli, R. D. Rogers, *J. Chem. Soc. Dalton Trans.* **1999**, 931.
[30] W. R. Dawson, J. L. Kropp, M. W. Windsor, *J. Chem. Phys.* **1966**, *45*, 2410.
[31] N. Sabbatini, M. Guardigli, A. Mecati, V. Balzani, R. Ungaro, E. Ghidini, A. Casnati, A. Pochini, *Chem. Commun.* **1990**, 878.
[32] B. Alpha, R. Ballardini, V. Balzani, J.-M. Lehn, S. Perathoner, N. Sabbatini, *Photochem. Photobiol.* **1990**, *52*, 299.
[33] R. S. Dickins, D. Parker, A. S. de Souza, J. A. G. Williams, *Chem. Commun.* **1996**, 697.
[34] T. C. Schwendemann, P. S. May, M. T. Berry, Y. Hou, C. Y. Meyers, *J. Phys. Chem. A* **1998**, *102*, 8690.
[35] N. W. Alcock, P. R. Barker, J. M. Haider, M. J. Hannon, C. L. Painting, Z. Pikramenou, E. A. Plummer, K. Rissanen, P. Saarenketo, *J. Chem. Soc. Dalton Trans.* **2000**, 1447.
[36] J. N. Demas, G. A. Crosby, *J. Phys. Chem. A* **1971**, *75*, 991.
[37] K. Nakamura, *Bull. Chem. Soc. Jpn.* **1982**, *55*, 2697.
[38] S. R. Meech, D. Phillips, *J. Photochem.* **1983**, *23*, 193.
[39] A. Altomare, G. Cascarano, C. Giacovazzo, A. Guagliardi, *J. Appl. Crystallogr.* **1993**, *26*, 343.
[40] P. T. Beurskens, G. Beurskens, W. P. Bosman, R. de Gelder, S. Garcia-Granda, R. O. Gould, R. Israel, J. M. M. Smits, Program system, Crystallography Laboratory, DIRDIF, University of Nijmegen (The Netherlands), **1996**.
[41] G. M. Sheldrick, SHELXTL Ver. 5, Bruker AXS, Madison WI (USA), **1995**.
[42] A. L. Spek, *Acta Crystallogr. Sect. A* **1990**, *46*, C34; A. L. Spek, PLATON, A Multipurpose Crystallographic Tool, Utrecht University, Utrecht, The Netherlands, **1998**; L. J. Farrugia, *J. Appl. Crystallogr.* **1999**, *32*, 837.

Received: June 24, 2002 [F4198]

  0947-6539/02/0824-5771 $ 20.00+.50/0